ELSEVIER

Journal of Photochemistry and Photobiology A: Chemistry 146 (2001) 109–119

Journal of Photochemistry and Photobiology A:Chemistry

www.elsevier.com/locate/jphotochem

Enhanced photocurrent generation and photooxidation of benzene sulfonate in a continuous flow reactor using hybrid TiO_2 thin films immobilized on OTE electrodes

Satoshi Horikoshi [a], Youko Satou [a], Hisao Hidaka [a,*], Nick Serpone [b]

[a] *Frontier Research Center for the Global Environment Protection (EPFC), Meisei University, 2-1-1 Hodokubo, Hino, Tokyo 191-8506, Japan*
[b] *Department of Chemistry and Biochemistry, Concordia University, 1455 de Maisonneuve Blvd. West, Montréal, Que., Canada H3G 1M8*

Received 20 April 2001; received in revised form 16 August 2001; accepted 19 September 2001

Abstract

The enhancement of photocurrent and photodegradation of organic pollutants was investigated using hybrid TiO_2 thin films prepared by a combined paste/sol–gel technique to immobilize the TiO_2 particles onto optically transparent electrodes (OTEs); they were connected in series in a continuous flow, bench-top, two-compartment photoreactor. The benzene sulfonate (BS) of the model substrate surfactant used was photodegraded in aqueous media to test the efficacy of the TiO_2/OTE electrode preparation and the construction of the photoreactor. Results indicate that the hybrid TiO_2 film/OTE electrodes were more efficient than either the pasted TiO_2/OTE electrode or the sol–gel TiO_2/OTE electrode for the photodegradation of BS, as evidenced by the evolution of carbon dioxide and the photocurrent generated. The extent of ring opening and generated photocurrent during the photodegradation of BS with the hybrid (HY) electrode was correlated to the pasted TiO_2 electrode and to the number of dip-coatings in the sol–gel. High photocurrents were generated in the cylindrical large photoreactor under continuous flow of the aqueous BS solution. Optimization of experimental factors for optimal efficiency of the setup was addressed with regard to the preparation of the HY electrodes, and to their size and location in the photoreactor.

Keywords: Titanium dioxide; Semiconductor electrode; Photocurrent; Photooxidation; Photodegradation

1. Introduction

The photocatalytic remediation of air and water ecosystems has been examined extensively by several workers. Practical applications of heterogeneous photocatalysis to air purification are under active scrutiny on a relatively large scale. By comparison, wastewater treatment on a similar scale has been surprisingly silent. Several issues have impeded progress in the latter: (i) the profusion and complexity of the chemical structures of wastewater contaminants, not least of which are the relatively high concentrations encountered in real-world wastewaters; (ii) the need for removal of TiO_2 catalyst particulates through costly filtration and/or centrifugation methods; and (iii) the necessity for continuous agitation to promote adsorption on the TiO_2 surface and to enhance UV light absorption. As a result, the development of highly reactive photocatalysts and two-dimensional immobilization of TiO_2 particles on a suitable support seemed desirable. To resolve some of these issues, optically transparent electrodes (OTEs) loaded with a hybrid TiO_2 thin film (henceforth referred to as HY TiO_2/OTE electrodes) were prepared by repeated sol–gel coating on a TiO_2 film in which the particles were pasted on the OTE electrode. The photoelectrochemical degradation of organic substances by means of TiO_2 film electrodes prepared by a paste (PA) procedure [1–7], a sol–gel (SG) method [8–14], a laser deposition method, MOCVD [15], and by a Ti-firing technique [16] has been reported.

There are advantages and disadvantages in the several procedures used to bind TiO_2 particles on an OTE glass to construct a suitable electrode. Typically, highly photocatalytic films show loss of TiO_2 from some of the TiO_2/OTE electrodes with consequential decrease in generated photocurrent. Though the TiO_2 thin film prepared by the SG method showed excellent characteristics without loss of metal-oxide particulates, the photocatalytic activity and the kinetics of photodegradation were disappointingly low, as were those when the TiO_2 films were prepared by laser-flash deposition (or the MOCVD). This study focused on three major strategies to achieve optimal efficiency:

* Corresponding author.
E-mail address: hidaka@epfc.meisei-u.ac.jp (H. Hidaka).

1010-6030/01/$ – see front matter
PII: S1010-6030(01)00595-0

1. *Preparation of a hybrid, active TiO_2/OTE electrode with high photoconversion efficiency*. Our efforts were specifically focused on designing a photoreactor setup that would enhance photooxidation of environmental contaminants in wastewaters, and achieve improved photocurrent generation. Relatively little has been done in this regard. To realize these desirable goals, we revisited some of the immobilization procedures used to prepare OTE electrodes so that we could control their fabrication and test them under our experimental conditions.
2. *Evaluation of TiO_2-fixation methods with high retention of TiO_2 particles*. Preliminary work using repetitive methods showed that immobilizing highly active TiO_2 (Degussa P-25 titania) onto OTE was not a suitable approach. Accordingly, another approach was taken which involved a silica sol to fix TiO_2. Unfortunately, this approach also turned out to be unsuitable as the photocatalytic activity of the TiO_2 declined considerably. Consequently, we sought other approaches. In our attempts, we noted that new photocatalysts had been developed by combining two semiconductor systems, each with a different bandgap. For example, such combinations as CdS/TiO_2 [17–19], CdS/ZnO [17,20], CdS/AgI [18], Cd_3P_2/ZnO [21], ZnO/ZnS [22], ZnO/ZnSe [23], AgI/Ag_2S [24] and CdS/HgS [25] have proven very effective. Methods to improve efficiencies for the photodegradation of phenol, 2-chlorophenol and pentachlorophenol using a composite of TiO_2, CdS, WS_2, FeO_3, SnO_2, WO_3 and ZnO specimens have also been described [26]. To our knowledge, immobilizing two differently prepared TiO_2 particulate systems by different methods on an OTE electrode has not been examined.
3. *Exploratory fabrication of a bench-top scale photoreactor with a string of connected HY TiO_2/OTE electrodes used in a continuous flow mode*. Photooxidation of organic pollutants and generation of photocurrent in large quantity were examined using highly efficient HY electrodes by fabricating a relatively large bench-top scale twin-cell photoreactor. The aqueous BS solution was circulated through the photoreactor in a continuous flow mode using a peristaltic pump.

The fabricated HY TiO_2/OTE electrodes and the photoreactor setup proved to be an overall excellent strategy to enhance the efficiency of photooxidation and to generate high photocurrent.

2. Experimental

2.1. Materials and reagents

Benzene sulfonate (BS: 0.l mM) of a surfactant model used to evaluate the various TiO_2/OTE electrodes was supplied by Tokyo Kasei Co. Ltd. The supporting electrolyte was aqueous NaCl solution (0.1 M). The active TiO_2 sample was supplied by Degussa (titania: P-25; specific surface area: $53\,m^2\,g^{-1}$ by BET measurements; particle size: 20–30 nm by TEM observation; ca. 78% anatase; 22% rutile by X-ray diffraction). The OTE (OTE: SnO_2-coated sodalime glass; neat resistance: $5.6\,W\,cm^{-2}$; film thickness of SnO_2: 960 nm) used to prepare TiO_2/OTE plates was a gift from Asahi Glass Co. Ltd. The dimensions of the OTE plate were 2 cm × 4 cm; an area of 2 cm × 3 cm (6 cm^2) of the glass was covered by TiO_2 particles for each of the immobilization methods used to fabricate the TiO_2/OTE electrodes.

2.2. Preparation of TiO_2-loaded OTE electrodes

Paste method (*PA*). A colloidal dispersion containing TiO_2 particles (P-25; loading: 100 mg) in ion-exchanged water (50 ml) was used as the source of titania. The dispersion was brushed onto the OTE glass plate, followed by drying and sintering the TiO_2/OTE glass combination electrode in an electric furnace at 400 °C (5 °C min^{-1}) for 1 h.

Sol-gel method (*SG*). Titanium tetraisopropoxide (28.4 g), diethanolamine (21.0 g) and ethanol (200 ml) were mixed under an inert atmosphere in a glove box that had appropriately been pre-purged with dry nitrogen gas. Subsequently, a solution of ethanol (4.6 g) and water (18 g) was added to the mixture under agitation for 1 h at ambient temperature, which led to the formation of a sol–gel. Lastly, ethanol was added four times to the sol–gel solution before dip-coating the OTE glass. The TiO_2-coated OTE glass was then dried at 50 °C for 2 min in air, and then heated at 400 °C for 1 h. The experimental operation of coating, drying and heating was repeated five times to give the thickest TiO_2 film.

Hybrid method (*HY*). This method consisted of fabricating the PA electrode, followed by dip-coating this electrode in the sol–gel solution. The dip-coating rate was $4\,mm\,s^{-1}$. After each dip-coat, the TiO_2/OTE glass was heated at 400 °C for 1 h. The sol–gel coating was repeated several times as desired. The photocatalytic activities of the resulting HY TiO_2/OTE electrodes were assessed by the extent of the photodegradation of the test substrate BS.

2.3. Analytical measurements

The photoreactor used to evaluate the various methods for binding TiO_2 onto the OTE glass consisted of two concentric Pyrex compartments divided into two layers with a glass plate [3]. The aqueous BS solution (0.1 mM, 50 ml) containing NaCl (100 mM) as the supporting electrolyte was magnetically stirred with a stirrer placed in the bottom of the working electrode compartment. The reactor was sealed with a Teflon septum through which were placed the electrodes and the salt bridge connected to the Ag/AgCl reference electrode via a KCl solution. The TiO_2/OTE electrode and the salt bridge composed the working electrode. The upper part of the salt bridge was near the TiO_2 surface. Only the portion of the TiO_2-coated working electrode was immersed in the solution. The counter electrode consisted of a platinum plate (2 cm × 2 cm). The TiO_2/OTE working

electrode, the Pt counter electrode, and the Ag/AgCl reference electrode were then connected to a BAS CV-50 W voltametric analyzer to control the potential at the TiO_2 surface and to measure the current between the TiO_2/OTE and Pt electrodes. Unless noted otherwise, the irradiation source was a Toshiba 75 W Hg lamp placed such that UV radiation was incident to the front side of the TiO_2/OTE electrode. The electrode was kept under an applied anodic bias of +0.3 V. The light irradiance was 12.5 mW cm^{-2} at wavelengths between 320 and 400 nm (maximum irradiance at 360 nm).

The large-scale cylindrical photoreactor consisted of TiO_2-fixed OTE glass electrodes defining the geometry illustrated in Fig. 1. The light source was a Hg lamp placed in the center of the reactor; it provided a light irradiance of 10.2 mW cm^{-2} illuminating outward from the center. The BS solution (BS: 0.1 mM; NaCl: 0.1 M) was continually circulated through the reactor at a rate of 100 ml min^{-1} with a peristaltic pump. The temperature of the solution was maintained at 25 °C with a cooling vessel placed outside the reactor. Each of the TiO_2/OTE electrodes was connected with a stainless steel guide. The Pt cathode plate (2 cm × 2 cm) was set beside the solution outlet. Two Ag/AgCl reference electrodes were placed facing the TiO_2/OTE electrodes. A black light (15 W) having a light irradiance of 3.0 mW cm^{-2} was also used as a light source for UV-irradiation.

Scanning electron micrographs (SEMs) were taken with a JEOL JSM-5200 electron microscope. The ratio

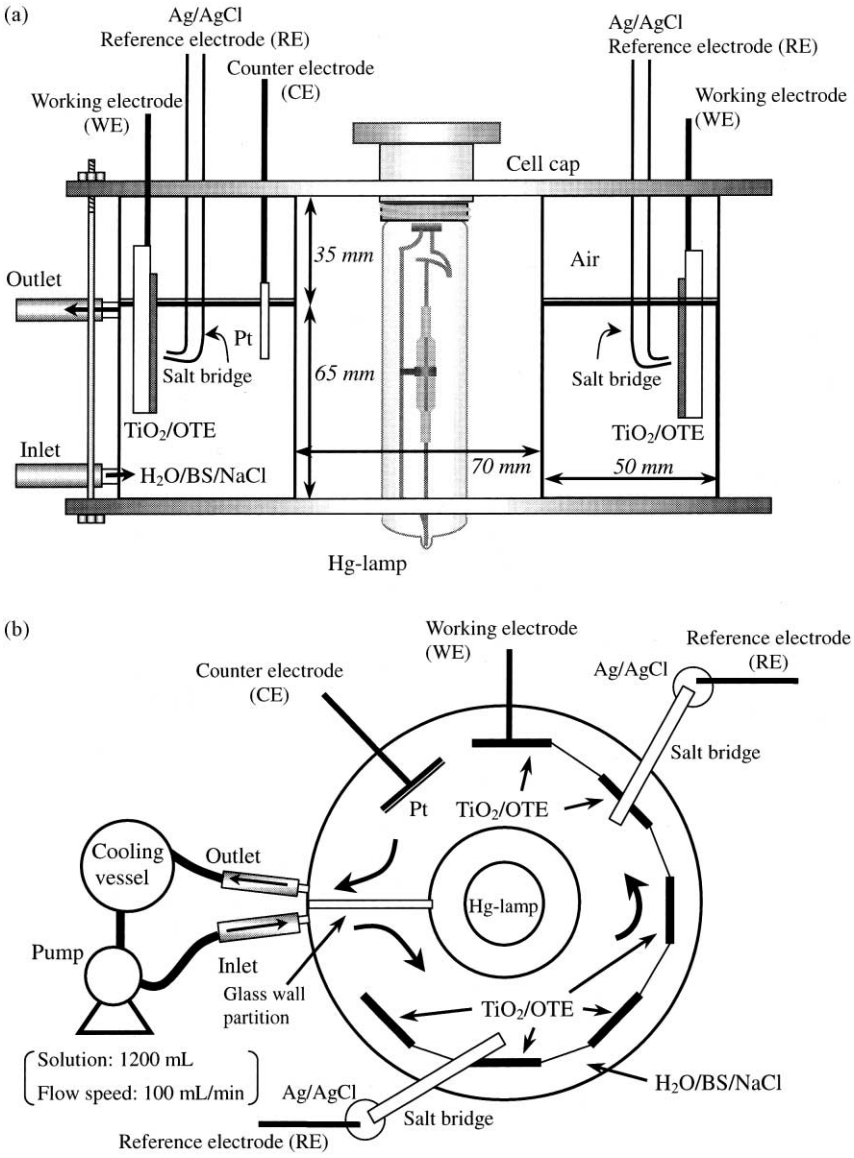

Fig. 1. Experimental setup of the photoreactor: (a) horizontal cross-section of the equipment with the Hg lamp located in the center of the cylinder; (b) top view of the setup. The six TiO_2/OTE electrodes are set around the lamp as indicated; a barrier was placed so as to allow flow of the solution from the inlet to the outlet. Note that the maximal flow rate possible in the peristaltic pump used was 100 mL/min. This allowed the solution to flow uniformly throughout the reactor. At a slower flow rate, for example at 50 mL/min, the solution flowed only close to the lamp as determined by a special dye solution.

of crystalline type (anatase/rutile ratio) for TiO_2 was obtained with a Rigaku Rad-B X-ray diffractometer (XRD). An UV–visible spectrophotometer (JASCO V-570 UV/VIS/NIR) measured the disappearance of the benzene ring absorption during the photodecomposition of the BS substrate. The contact angle between a drop of H_2O or of the BS solution and the TiO_2/OTE electrode was analyzed with a CA-W150 automatic contact angle meter (Kyowa Interface Science Co. Ltd.). The quantity of $^{\bullet}OH$ radicals formed was assessed relative to a standard Mn^{2+} marker ion using a JEOL JES-TE200 ESR spectrometer.

2.4. Photocurrent and photodegradation

The photocurrent was generated by applying a potential bias to the TiO_2 electrode. UV illumination (wavelengths < 387 nm for anatase) of the electrode generates electron/hole pairs, which subsequent to separation yields conduction band electrons (e^-_{CB}) and valence band holes (h^+_{VB}), identical to the events that occur in dispersion (Eq. (A)). The holes are subsequently trapped by HO^- ions (or by H_2O) to yield $^{\bullet}OH$ radicals (and H^+; Eq. (B1)). These radicals readily oxidize organic pollutants and subsequent intermediates formed during the mineralization process to carbon dioxide. Our data do not preclude the possibility that they are also degraded by direct oxidization (Eqs. (B2) and (B3)). However, concentration differences suggest that $^{\bullet}OH$ radical oxidation should predominate. The inception of electrons (e^-) generates a photocurrent (Eq. (C1)). A small quantity of superoxide radical anions $O^{\bullet-}_2$ may also form on the outer surface of the TiO_2 film that faces the bulk solution. These radicals can interact with protons under acidic conditions to produce $^{\bullet}OOH$ radicals (Eq. (C2)). These too are reasonably good oxidizing agents. The schematic diagram of Fig. 2 illustrates the details of the setup for photocurrent generation.

$$TiO_2 + h\nu \rightarrow TiO_2\,(e^-_{CB} + h^+_{VB}) \quad \text{(A)}$$

$$h^+_{VB} + (H_2O)_{ads} \rightarrow H^+ + {}^{\bullet}OH\ (\text{strong oxidizing species}) \quad \text{(B1)}$$

$$h^+_{VB} + (RH)_{ads} \rightarrow H^+ + R^{\bullet} \rightarrow\rightarrow (\text{Intermediates; Int})_{ads} \quad \text{(B2)}$$

$$h^+_{VB} + (\text{Int})_{ads} \rightarrow H^+ + (\text{Int})^{\bullet} \rightarrow\rightarrow \text{mineralization} \quad \text{(B3)}$$

$$e^-_{CB} \rightarrow e^-_{OTE} \rightarrow \text{photocurrent} \quad \text{(C1)}$$

$$e^-_{CB} + (O_2)_{ads} \rightarrow (O^{\bullet-}_2)_{ads} \xrightarrow{H^+} {}^{\bullet}OOH\ (\text{strong oxidation species}) \quad \text{(C2)}$$

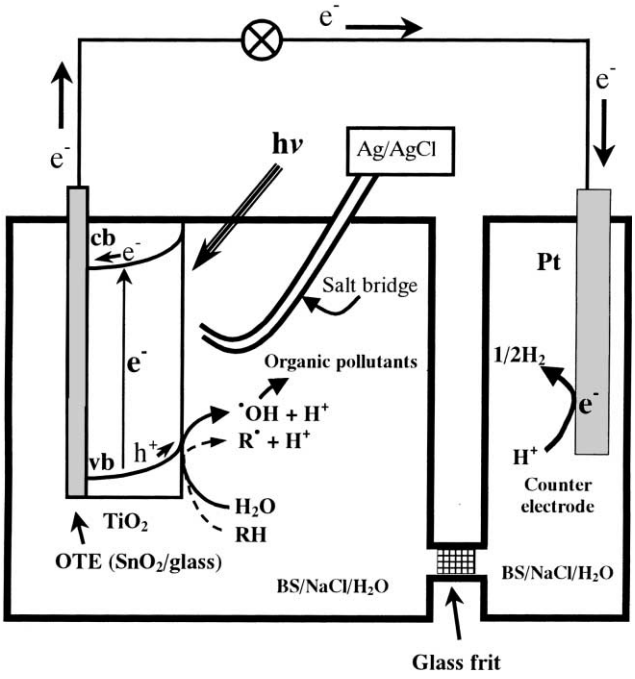

Fig. 2. Schematic illustration of the photoreactor system setup to generate photocurrent.

3. Results and discussion

3.1. Evaluation of the TiO_2/OTE photoelectrodes

3.1.1. Surface morphology of electrodes

SEM of the surface of the various TiO_2/OTE electrodes prepared by the PA, SG and HY methods are illustrated in Fig. 3(a), (b) and (c), respectively. The surface morphology of the PA TiO_2/OTE electrode consisted of several tiny cavities as shown in Fig. 3(a-1). The surface imperfections of the electrode were confirmed by further magnification (Fig. 3(a-2)) to reveal aggregates of TiO_2 nanoparticles and deep crevasses in the SEM image. The width of the crevasses was ca. 1000 nm; this can cause irregular light reflection and scattering of the UV light ($\lambda = 387$ nm). The SEM micrograph for the sol–gel TiO_2 photoelectrode shown in Fig. 3(b-1) and (b-2) reveals large heterogeneities in the surface topology with relatively large cracks/pores. By contrast, the surface of the photoelectrode prepared by the HY method was relatively smooth and flat in which the crevasses and imperfections were filled or covered with a sol–gel membrane (see Fig. 3(c-1)).

The preparation of TiO_2-fixed electrodes by the PA and SG methods proved to be rather difficult to achieve a relatively flat surface, subsequent to drying and sintering the TiO_2 particulates onto the OTE glass plate. The surface morphology of the HY electrode was flat and porous. The crystalline structures of titanium dioxide on the TiO_2/OTE electrodes are listed in Table 1, as estimated according

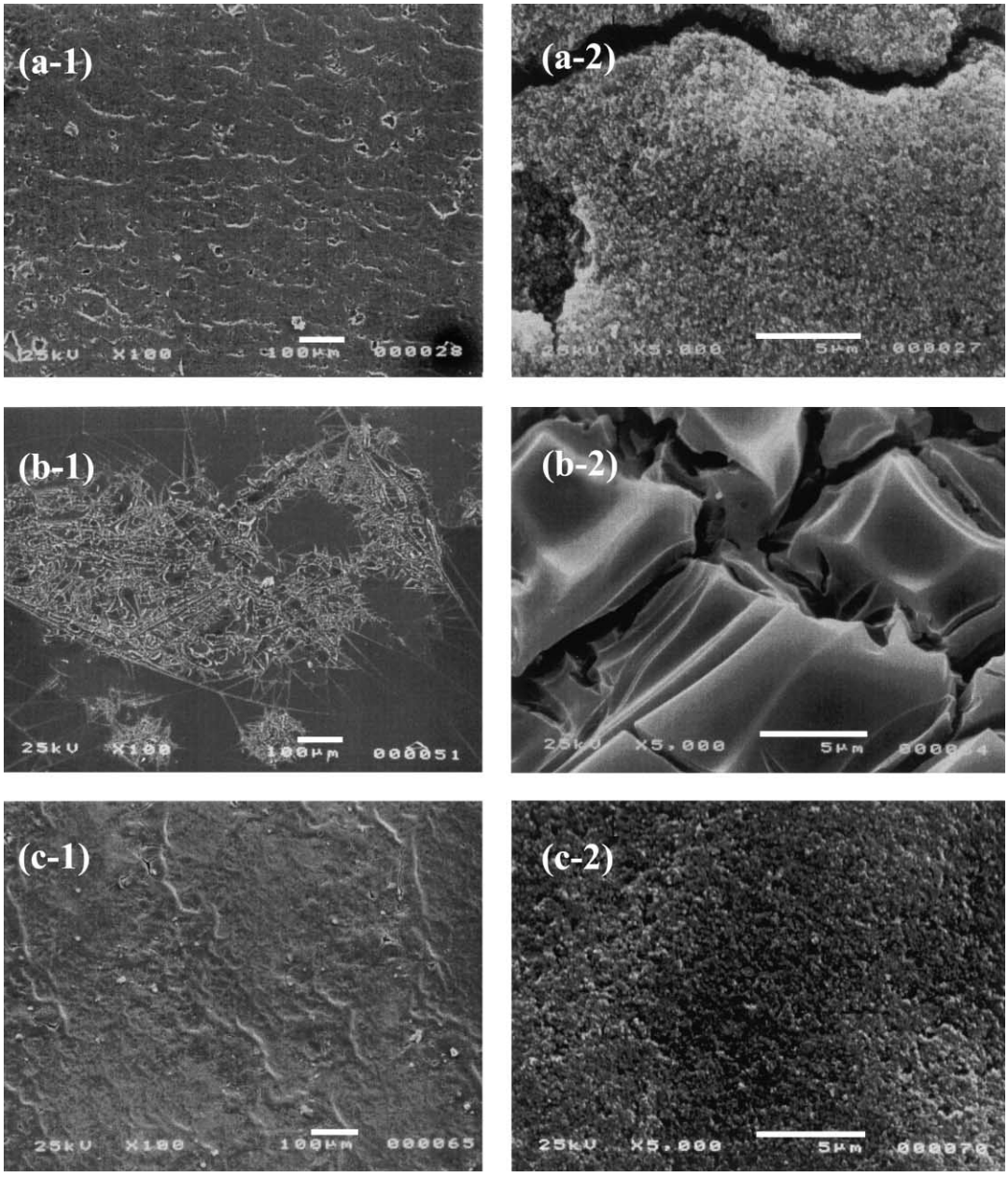

Fig. 3. Surface morphologies of TiO_2/OTE electrodes by SEM microscopy. Electrodes were prepared by: (a-1 and a-2) the PA technique; (b-1 and b-2) SG technique; (c-1 and c-2) HY technique. Magnifications of the SEM micropgraphs were: (1) 100× (left); (2) 5000× (right).

to Eq. (1):

$$\text{anatase}\ (\%) = \frac{100}{1 + 1.265(I_{\text{rutile}}/I_{\text{anatase}})} \quad (1)$$

Table 1
Percent of crystalline form of TiO_2 particulates on the TiO_2/OTE electrodes determined from the XRD patterns

Preparation procedure	Anatase (%)	Rutile (%)
PA	77.8	22.2
SG	100	0
HY	84.3	15.7

where I_{rutile} and I_{anatase} are the intensities of the corresponding XRD signals at $2\theta = 27.42^\circ$ for the rutile and 25.28° for the anatase, respectively.

It is clear from the data of Table 1 that the PA procedure change nothing in the anatase/rutile ratio in the Degussa P-25 TiO_2 particles immobilized on the OTE glass plate. The SG method of preparing titanium dioxide yields 100% anatase, and after dip-coating the OTE plate several times followed by drying and sintering caused no changes in the relative content of the anatase polymorph. However, when the HY method was used (PA then SG coating) the XRD pattern showed a slightly greater quantity of the anatase form

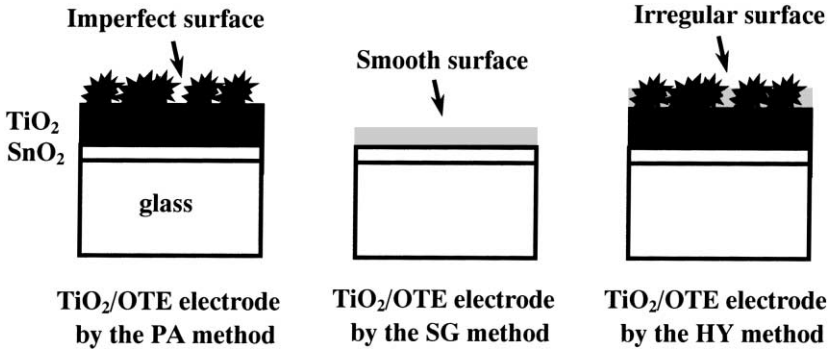

Fig. 4. Cartoons illustrating the presumed features of the TiO_2-deposited surface for the PA electrode (left), SG electrode (middle), and HY electrode (right).

(84.3% anatase versus 15.7% rutile) in the HY TiO_2/OTE electrode surface. This shows that the sol–gel TiO_2 membrane did not completely cover the particles immobilized on the OTE glass by the PA method. The cracks and/or cavities of the TiO_2 film prepared by the PA procedure were filled by the sol–gel titania particles. However, complete covering of the surface did not occur over the whole surface of the thin film as summarized in the cartoons of Fig. 4. In the HY electrode, there remained islands of P-25 TiO_2 particles protruding over the smooth surface of the HY electrode. No doubt these P-25 TiO_2 particles may be the cause for the efficient photocatalytic degradation displayed by these HY electrodes.

3.1.2. Photodegradation of BS

The various HY TiO_2/OTE electrodes were compared to each other and to the PA and SG electrodes with respect to their efficiencies in the photodegradation of BS as indicated by the decrease of the relevant absorption band of the benzene moiety in the UV region, and by the magnitude of the photocurrent generated (see Fig. 5). The four HY TiO_2/OTE electrodes tested are denoted by the quantity of TiO_2 used, namely 2.5 or 5 mg, and the number of times that the PA electrode was dip-coated in the sol–gel titania. For example, HY(5/5) stands for a TiO_2/OTE electrode containing 5 mg of TiO_2 which was then dipped into the sol–gel titania five times.

The disappearance of the benzene ring absorption, the temporal variation of the photocurrent, and the temporal increase in the number of coulombs produced in the photodegradation of BS (0.1 mM, 50 ml) using the PA, SG and HY TiO_2/OTE electrodes at a constant bias of +0.3 V are illustrated in Fig. 5(a), (b) and (c), respectively. Under our experimental conditions, the efficiency of photodegradation of the test substrate is HY(5/5) ∼ HY(5/2) ∼ HY(2.5/5) > HY(2.5/2) > PA > SG after a 6-h irradiation period. In all cases, the HY electrodes were more efficient than either the PA or SG electrode. Evidently, the sol–gel dip-coatings of the PA TiO_2/OTE electrode led to a significant improvement in the photooxidation rate. Initially the magnitude of the photocurrent generated was in the order HY(5/5) ∼ HY(2.5/5) ∼ HY(5/2) > SG > HY(2.5/2) ≫ PA within 1 h of irradiation; after 3.5 h of illumination, the HY(2.5/2) and the SG electrodes switched positions in this order. After 6 h of UV-irradiation, the order in photocurrent efficiency was HY(5/5) > HY(2.5/5) ∼

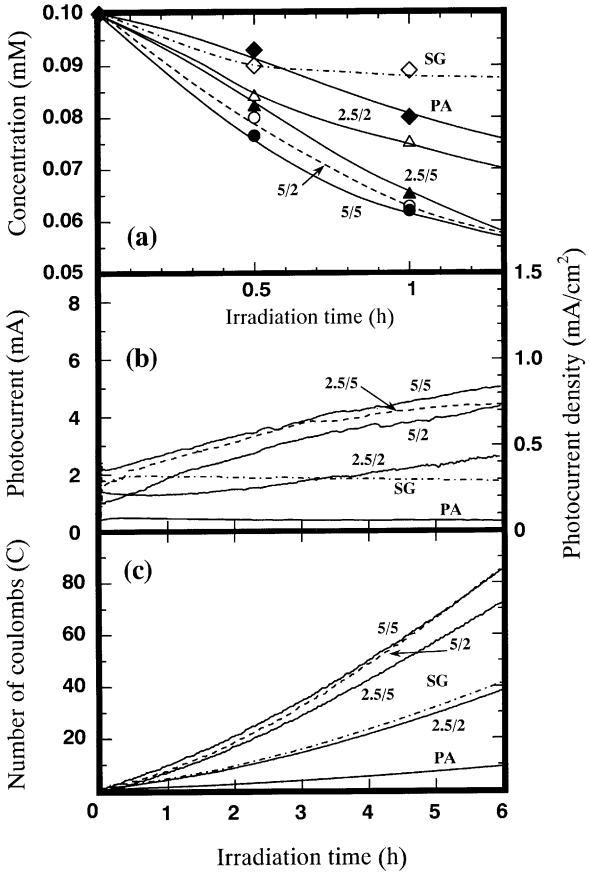

Fig. 5. (a) Temporal loss of the benzene moiety in BS, (b) temporal variations of photocurrent, and (c) increase in the number of coulombs with time in the photodegradation of BS (0.1 mM, 50 ml) using the PA. SG and HY TiO_2/OTE electrodes under an applied bias of +0.3 V. The notation of the HY electrodes is given by (milligrams of TiO_2 particles pasted on OTE) (number of sol–gel dip-coatings); for example HY(5/5) stands for a TiO_2/OTE electrode containing 5 mg of TiO_2 dipped into the titania sol–gel five times.

Table 2
Percent of TiO_2 remaining on TiO_2-fixed OTE electrodes after agitation for 15 h

	PA	SG	HY(5/5)	HY(5/2)	HY(2.5/5)	HY(2.5/2)
Retention (%)[a]	93.5	∼100	98.8	98.0	99.0	98.5

[a] 100 − [(weight after 15 h − stirring)/initial weight] × 100.

HY(5/2) ≫ HY(2.5/2) > SG ≫ PA. Differences in the six electrodes examined are even more evident by the ratio of the number of coulombs produced after the 6-h irradiation period: HY(5/5):HY(5/2):HY(2.5/5):SG:HY(2.5/2):PA = 9.1:9.1:7.7:4.3:4.1:1. Evidently, the PA TiO_2/OTE electrode dipped twice in the sol–gel solution (i.e. HY(2.5/2)) yields the same quantity of coulombs as the naked SG electrode, and HY(5/5) and HY(5/2) electrodes are equally efficient in this regard. Photocurrent generation with an HY TiO_2/OTE electrode increased with increasing UV-irradiation time. By contrast, for the PA and SG TiO_2/OTE electrodes longer irradiation times had no effect on the generated photocurrent. The increase in photocurrent with the HY TiO_2/OTE electrodes is likely due to a facile adsorption/desorption of BS and its intermediates on the TiO_2 surface. Note that our data do not preclude possible contributions from photocurrent doubling as might occur during the photodegradation of intermediates. With respect to the rate of decrease of the UV-absorption of BS, the ratio in the order of the electrodes described above is 5.6:5.0:4.5:1.0:1.9:1.5 after 6 h of UV-irradiation. It is clear that the influence of the various HY preparative methods is felt more in the electric current and in the photocurrent generated than in the rate of photooxidation of BS. Ring opening of the BS structure and the photocurrent generated indicate that the HY electrodes are more effective than either the PA and SG electrodes. The results also suggested that the HY(5/5) electrode was the better choice for further study. It is also relevant to note that an HY TiO_2 electrode, for which the surface contains no cracks or grooves, minimizes light scattering and consequently enhances light absorption and improves efficiencies. The number of coulombs generated from the HY(5/5) electrode in water in the absence of BS was 20 after 6 h of irradiation, whereas the number was 85 in the presence of BS for the same irradiation period. This infers that an intermediate may be involved in photocurrent generation in the photooxidation of BS by the HY electrode.

3.1.3. Integrity of the electrodes

The loss of TiO_2 particles from TiO_2/OTE electrodes is an important factor in any fabrication of electrodes and in any method used to immobilize TiO_2 as these methods might affect the ensuing properties. Such loss of TiO_2 from the TiO_2/OTE thin film electrode, as might occur under magnetic agitation for long periods of time, would impair repeated usage of the electrodes. Consequently, we examined the retention of TiO_2 on the TiO_2/OTE electrodes by carrying out experiments, under otherwise identical conditions, in water under magnetic agitation and irradiation for 15 h. Results are given in Table 2. They show that substantive loss (6.5%) of TiO_2 occurred in the PA electrode, none in the SG electrode, and <1–2% in the HY fabricated electrodes.

The various contact angles between the PA, SG and HY electrodes and a drop of H_2O (or BS solution) determined under a power density of 1 μW cm^{-2} are displayed in Fig. 6. The ratio between the average contact angle (ACA) for each fabricated electrode relative to the SnO_2 base of the OTE glass in water was 0.103, 0.385 and 0.174 (ACA to ACA-SnO_2), respectively. The PA TiO_2-fixed electrode showed the greatest affinity to water, i.e. the PA electrode surface was more hydrophilic than either the SG or HY electrode surface. As noted earlier, the sol–gel dip-coating did not cover the entire surface of the PA electrode. Consequently, the HY electrode is also somewhat hydrophilic, albeit less than the PA electrode. By contrast, the SG electrode was the least hydrophilic.

Measured contact angles in the BS solution were different from the results obtained in water. The corresponding contact angle ratios relative to SnO_2 were 0.089, 0.392 and 0.069 for the PA, SG and HY electrodes, respectively. Clearly, the HY electrode displayed the greatest affinity for water in the BS solution, and accordingly the HY electrode surfaces were the most hydrophilic. These observations are consistent with the greater magnitude of photocurrent generated from the BS solution (Fig. 5(b)). The greater efficiency of the photodegradation of BS using the HY TiO_2-fixed electrodes relative to the PA and SG electrodes is due to a greater adsorption of BS on the TiO_2 surface.

If the photodegradation of organic pollutants were solely governed by the number of •OH radicals photogenerated on the TiO_2 film surface, then the efficiency of the photodegradation of BS would be expected to follow a trend identical to that of the concentration of such radicals. As well, the more efficient the photodegradation the greater the photocurrent generated should be. Formation of •OH radicals by illumination of the PA, SG and HY(5/5) electrodes in water (20 ml) in the absence of BS was monitored by DMPO (15 μl) spin-trap ESR techniques (see Fig. 7) in a Pyrex rector under magnetic agitation. It is evident that the concentration of •OH radicals produced from the irradiated electrodes varied as PA > HY > SG; the concentration ratio was, respectively, 3.5:2.8:1.0 after 60 min of UV illumination with a 75 W Hg lamp (light irradiance: 5.5 mW cm^{-2}). Note that the TiO_2-fixed electrode used for the ESR analysis were not under an applied bias. The data of Fig. 7 also demonstrate that the number of •OH radicals formed for each of the elec-

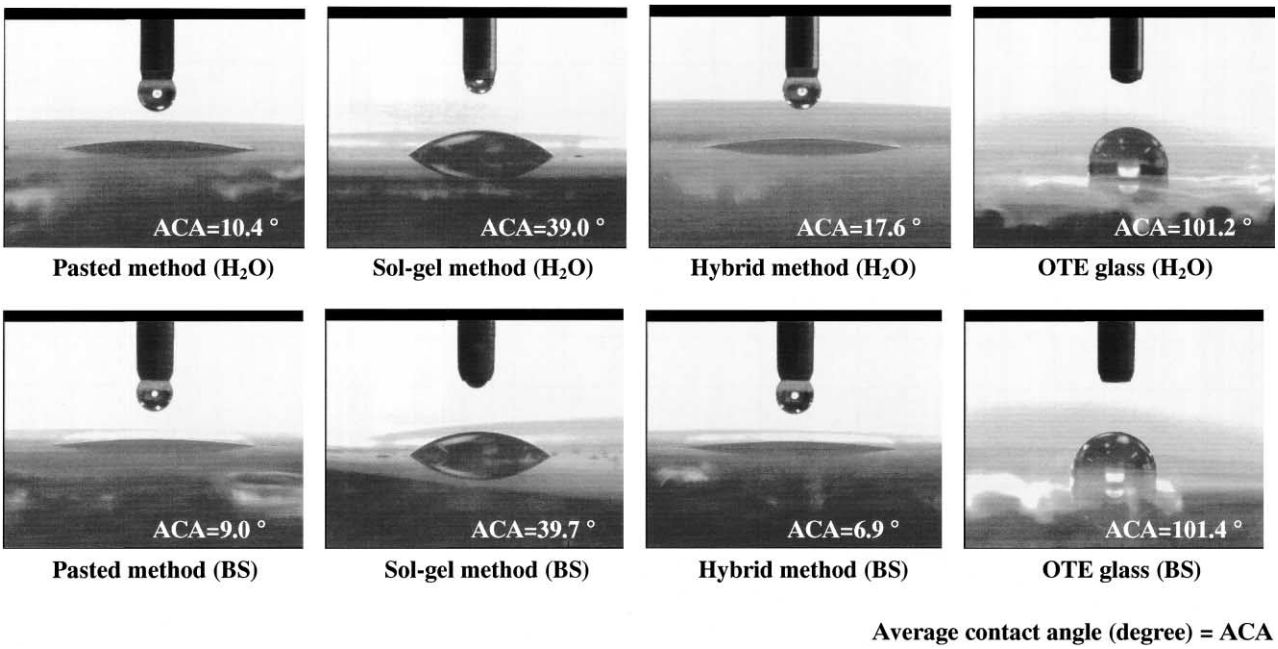

Fig. 6. Contact angles for a drop of water (top panel) and a drop of BS solution (0.1 mM, bottom panel) on the TiO_2/OTE electrode surface to examine the hydrophobicity/hydrophilicity of the various electrodes prepared by the PA, SG and HY techniques.

trodes does not correlate with the order of photodegradation of BS as evidenced by the rate of decrease of the appropriate absorption band of a BS solution, which corresponds to ring opening in BS. However, the order of the ratio does correlate with the results from contact angle measurements in water, i.e. with the extent of hydrophilic character of the electrode surface.

From the lack of correlation noted above, it is tempting to suggest that the direct photooxidation of BS by the valence band holes may also be a significant pathway in the degradation of BS. Many workers would argue in favor of this inference. Unfortunately, the concentration of •OH radicals, the hydrophilicity of the electrode surface, the crystalline structure of the particles at the electrode surface (anatase versus rutile), the extent of adsorption of the BS substrate, the topology of the electrode surface, among others, are only a few of the factors that govern the redox chemistry taking place at the particle/solution interface. There are several other factors that govern interfacial chemistry in particular, and interfacial phenomena in general, so that little can be said about the principal factor that governs surface oxidative or reductive chemistry [27].

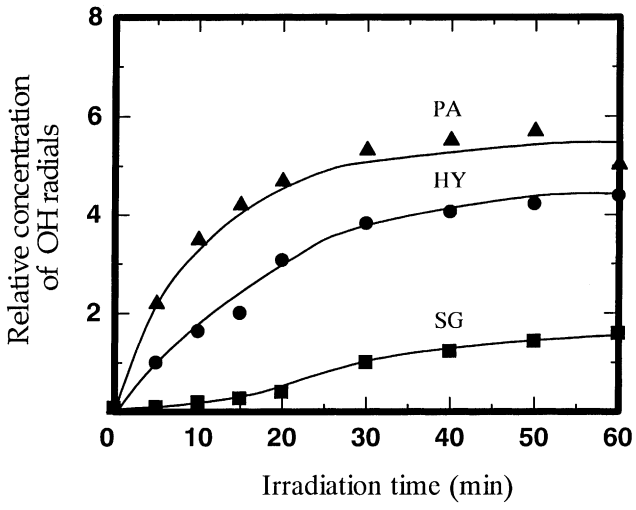

Fig. 7. Temporal formation of •OH radicals in a UV-irradiated aqueous solution monitored by ESR spectroscopic techniques using the DMPO spin-trap agent.

3.2. Photocurrent and photodegradation in a large-scale photoreactor

The photodegradation of BS and generation of photocurrent in an aqueous BS/NaCl solution in a large-scale photoreactor was examined under five different experimental conditions with regard to the size of the TiO_2/OTE electrodes and the position of these electrodes in the reactor. The details of the reactor/electrode configuration are illustrated in Figs. 1 and 8. The effect of the number of Ag/AgCl reference electrodes on the effectiveness of the photodegradation and photocurrent generation was examined with twin Ag/AgCl electrodes. All the TiO_2/OTE electrodes used were fabricated by the HY(5/5) method. The configurations and the number of electrodes employed are depicted in the five cartoons of Fig. 8. In the model M1 configuration, the six electrodes had total dimensions 2 cm × 4 cm (OTE glass) of which an area of 2 cm × 3 cm was covered with the

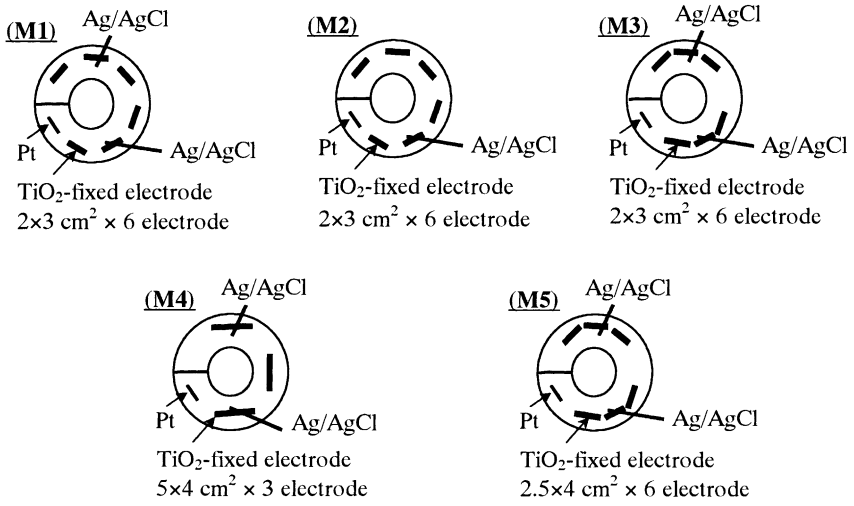

Fig. 8. Cartoons depicting the disposition of the TiO_2/OTE electrodes in the cylindrical photoreactor.

TiO_2 film. The electrodes were positioned as indicated in the cylindrical photoreactor together with the two Ag/AgCl electrodes (see Fig. 8). The model M2 was identical to model M1 except that only one Ag/AgCl reference electrode was used. Though the model M3 reactor was identical in size to M1, two pairs of three electrodes each were arranged as shown in Fig. 8; two Ag/AgCl reference electrodes were utilized. In the model M4, the TiO_2 film covered an area of 5 cm × 4 cm on a 5 cm × 5 cm OTE glass. Only three working electrodes were used in model M4. In model M5, the TiO_2 film covered an area of 2.5 cm × 4 cm of the OTE glass plate (2.5 cm × 5 cm). Six working electrodes were employed in model M5 with two reference electrodes; the configuration used was identical to that of model M3. The TiO_2 loading on each of the OTE glass plate for all models was 0.83 mg cm^{-2}. The total TiO_2 film area was 36 cm^2 in the M1, M2 and M3 models, and 60 cm^2 in the M4 and M5 configurations. The order of the total quantity of TiO_2 particles used was M1 = M2 = M3 ≪ M4 = M5, and the amount of TiO_2 about each electrode was M4 ≫ M5 > M1 = M2 = M3.

Comparison of the five configuration models of HY(5/5) TiO_2/OTE electrodes was made with respect to the extent of disappearance of the UV absorption band of BS and the magnitude of photocurrent generated, together with the number of coulombs produced (see Fig. 9). The order of ring opening of the BS structure for the five reactor configuration models was M5 ≫ M4 > M3 > M1 > M2; increase in photocurrent followed the order M5 ≫ M3 > M4 > M1 > M2 after 5 h of illumination. The effect of the number of Ag/AgCl reference electrodes used was evidenced by M1 and M2. Within experimental error, there was no change with respect to the photooxidation of BS. However, the photocurrent generated in model M1 was greater than in M2. Differences in the disposition of the six electrodes had no effect on the rate of photodecomposition of BS in M1 and M3. However, photocurrent generation was more efficient

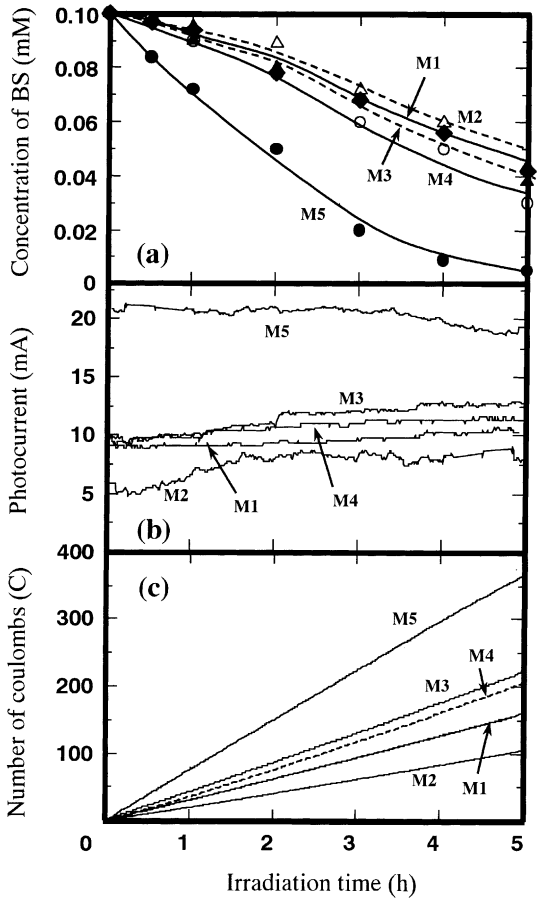

Fig. 9. (a) Temporal changes in the concentration of BS as evidenced by benzene ring cleavage using the five configurations, (b) temporal changes in the photocurrent generated during this photooxidation, and (c) temporal increase in the number of coulombs for the five configuration models of electrodes under an applied bias of +0.3 V in the large-scale photoreactor.

Table 3
Percent loss of UV absorption and photocurrent generated (C cm^{-2}) in the photooxidation of BS after an irradiation time of 5 h with the different dispositions of the TiO_2/OTE electrodes

	M1[a]	M2[a]	M3[a]	M4[b]	M5[b]
Loss of absorption intensity					
Percent loss[c]	58	56	62	70	95
Specific loss (% loss cm^{-2})	1.6	1.6	1.7	1.2	1.6
Coulombs (C cm^{-2})	4.4	2.9	5.5	3.4	6.2

[a] TiO_2 film area on OTE electrode = 36 cm^2.
[b] TiO_2 film area on OTE electrode = 60 cm^2.
[c] Percent loss in UV absorption band after 5 h (%) = 100 − {concentration(mM)/0.1 mM}.

when the TiO_2 electrodes were configured closer to each other as in M3. In other words, if the TiO_2/OTE electrodes in the photoreactor are placed closer to each other and if smaller electrodes are used, both the photodecomposition process and photocurrent generation become more efficient.

The intermediates produced from the photodegradation of BS are easily decomposed when the TiO_2/OTE electrodes are close to each other. The relationship between M1, M4 and M5 is noteworthy. The larger surface area TiO_2/OTE electrodes are more efficient for a given TiO_2 loading. Results also indicate that when the area of the electrode is small and a greater number of electrodes are used, efficiency is enhanced (e.g. compare M4 and M5 in Fig. 9). A reason for scaling-up the area of the TiO_2 film for a given TiO_2 loading was the increase in surface area of the film yielding a thinner electrode, which leads to decreased electrical resistance and to increased generation of photocurrent.

The extent of photooxidation and the photocurrent densities per area of the surface are summarized in Table 3. The specific percent loss of UV absorption band intensity per area of TiO_2 film surface was about the same for all configurations, except for M4 for which it was lower. The number of coulombs generated per area of electrode surface was in the order M5 > M3 > M1 > M4 > M3. The configuration model M5 was the most efficient in all respects as demonstrated by the results illustrated in Fig. 9.

Experiments were also carried out with the configuration model M5 to assess the decomposition of BS and the photocurrent generated using different irradiation sources: illumination with a black light versus illumination with the 75 W Hg lamp (see Section 2). Results of ring opening and photocurrent generated are illustrated in Fig. 10(a). Fig. 10(b) and (c) portray the temporal variations in photocurrent and the temporal concentration changes in BS (from UV spectral changes) normalized to 1 mW cm^{-2}.

The photodegradation of BS with the black light was 12-fold slower than with the Hg lamp, whereas the photocurrent was 2-fold smaller with the black light (Figs. 9 and 10(a)). The difference in light irradiance was about 3.4 times greater for the Hg lamp (10.2 mW cm^{-2}) relative to the black light (3 mW cm^{-2}). When normalized to 1 mW cm^{-2}, the

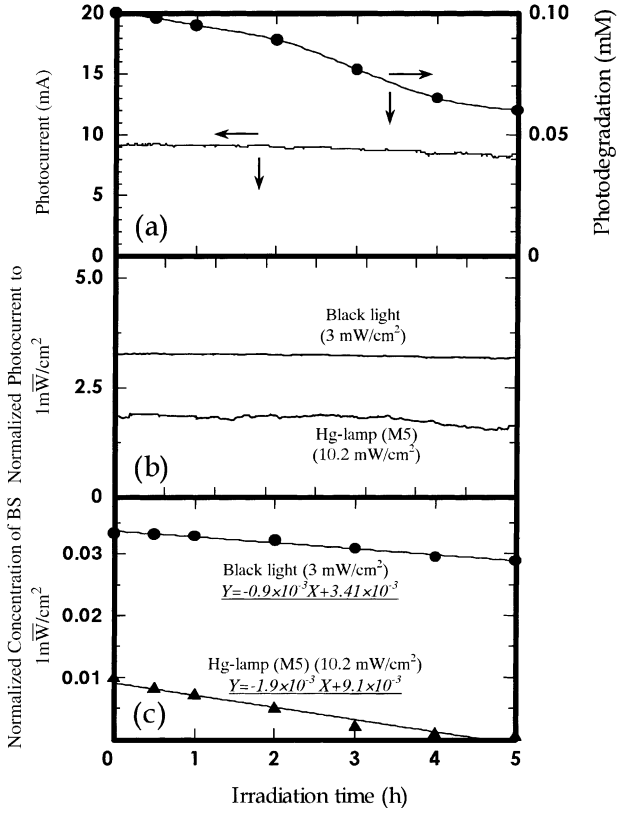

Fig. 10. (a) Disappearance of BS and photocurrent generated during the photooxidation of BS using the M5 configuration and a black light (3 mW cm^{-2}) as the irradiation source, (b) temporal changes in generated photocurrent normalized to 1 mW cm^{-2} using the Hg lamp and black light, and (c) temporal decrease of the concentration of BS also normalized to 1 mW cm^{-2} under illumination from either a Hg lamp or a black light.

photocurrent generated is greater for illumination with the black light than with the Hg lamp (see Fig. 10(b)). This infers that photocurrent generation during the photooxidation of BS is also significant at low light irradiance. Comparison of the degradation of BS, also normalized to 1 mW cm^{-2}, was noted by the variation in the slope of the linear relationships depicted in Fig. 10(c). The greater slope, which scales with the degradation efficiency, was seen by illuminating the M5 configured reactor with the Hg light source (slope −0.0009 for the black light versus −0.0019 for the Hg lamp). In this particular case and under the conditions used, we deduce that the Hg lamp is the light source of choice.

4. Summary

The hybrid fabrication method to prepare a TiO_2/OTE electrode from the combination of binding TiO_2 particles by the PA procedure followed by several dip-coatings in a sol–gel leads to a significant catalytic TiO_2/OTE electrode as a potentially new device for wastewater treatment and generation of photocurrent. The HY TiO_2/OTE electrode exhibits relatively interesting characteristics in terms

of photocatalytic activity, formation of •OH radicals from islands of P-25 TiO_2 particles above the sol–gel surface, and from the point of view that loss of TiO_2 particles from the OTE electrode surface is relatively small. No doubt the electrode surface morphology bears on the efficiencies of the processes examined. Although the HY TiO_2/OTE electrode exhibits a few cracks and imperfections, the photodegradation rate is nonetheless improved because of a decrease in light scattering at the electrode surface. Enhanced activity in photodegradation and photocurrent generation with the HY electrode is also due to improved adsorption of BS on the electrode. From our data presented herein, we deduce that an efficient TiO_2 large-scale reactor necessitates the following three features: (a) small electrodes; (b) a reactor configuration in which the electrodes are located as close to each other as possible; (c) for a given TiO_2 loading, thinner and larger area films are desirable. The photodecomposition of pollutants is made more efficient, and photocurrent generation is enhanced. Irradiation with a weak light source can also generate photocurrents. However, an irradiation source with greater light irradiance is desirable for the photodegradation. As well, large photoreactors possess excellent characteristics for photocurrent generation and photodegradation.

Acknowledgements

We are grateful to the Japanese Ministry of Education, Culture, Sports, Science and Technology (Grant-in-aid for Scientific Research No. 10640569 to HH), and to the Natural Sciences and Engineering Research Council of Canada (Ottawa; Grant No. A5443 to NS) for generous support of our work.

References

[1] H. Hidaka, Y. Asai, J. Zhao, K. Nohara, N. Serpone, E. Pelizzetti, J. Phys. Chem. 99 (1995) 8244.
[2] H. Hidaka, H. Nagaoka, K. Nohara, T. Shimura, S. Horikoshi, J. Zhao, N. Serpone, J. Photochem. Photobiol. A 98 (1996) 73.
[3] H. Hidaka, T. Shimura, K. Ajisaka, S. Horikoshi, J. Zhao, N. Serpone, J. Photochem. Photobiol. A 109 (1997) 165.
[4] K. Vinodgopal, S. Hotchandani, P.V. Kamat, J. Phys. Chem. 97 (1993) 9040.
[5] K. Vinodgopal, U. Stafford, K.A. Gray, P.V. Kamat, J. Phys. Chem. 98 (1994) 6797.
[6] K. Vinodgopal, P.V. Kamat, Environ. Sci. Technol. 29 (1995) 841.
[7] K. Vinodgopal, P.V. Kamat, Solar Energy 38 (1995) 401.
[8] G. Marci, L. Palmisano, A. Sclafani, A.M. Venezia, R. Campostrini, G. Carturan, C. Martin, V. Rives, G. Solana, J. Chem. Soc., Faraday Trans. 92 (1996) 819.
[9] D.H. Kim, M.A. Anderson, Environ. Sci. Technol. 28 (1994) 479.
[10] D.H. Kim, M.A. Anderson, J. Photochem. Photobiol. A 94 (1996) 221.
[11] I. Moriguchi, H. Maeda, Y. Teraoka, S. Kagawa, J. Am. Chem. Soc. 117 (1995) 1139.
[12] I. Moriguchi, H. Maeda, Y. Teraoka, S. Kagawa, Chem. Mater. 9 (1997) 1050.
[13] D.H. Kim, M.A. Anderson, Environ. Sci. Technol. 28 (1994) 479.
[14] P.A. Mandelbaum, A.E. Regazzoni, M.A. Blesa, S.A. Bilmes, J. Phys. Chem. B 103 (1999) 5505.
[15] G.K. Boschloo, A. Goossens, J. Schoonman, J. Electrochem. Soc. 144 (1997) 1311.
[16] Y. Maeda, M. Ichikawa, Y. Kudoh, Chem. Soc. Jpn. 3 (1997) 227.
[17] L. Spanhel, H. Weller, A. Henglein, J. Am. Chem. Soc. 109 (1987) 6632.
[18] K.R. Gopidas, M. Bohorquez, P.V. Kamat, J. Phys. Chem. 94 (1990) 6435.
[19] N. Serpone, E. Borgarello, M. Gratzel, J. Chem. Soc., Chem. Commun. (1984) 342.
[20] S. Hotchandani, P.V. Kamat, J. Phys. Chem. 96 (1992) 6834.
[21] L. Spanhel, A. Henglein, H. Weller, Ber. Bunsen-Ges. Phys. Chem. 91 (1987) 1359.
[22] J. Rabani, J. Phys. Chem. 93 (1989) 7707.
[23] P.V. Kamat, B. Patrick, J. Phys. Chem. 96 (1992) 6829.
[24] A. Henglein, M. Gutierrez, H. Weller, A. Fojtik, J. Jirkovsky, Ber. Bunsen-Ges. Phys. Chem. 93 (1989) 593.
[25] A. Haesselbarth, A. Eychimieller, R. Eichberger, M. Giersig, A. Mews, H. Weller, J. Phys. Chem. 97 (1993) 5333.
[26] N. Serpone, P. Maruthamuthu, P. Pichat, E. Pelizzetti, H. Hidaka, J. Photochem. Photobiol. A 85 (1995) 247.
[27] A.V. Emeline, A. Salinaro, N. Serpone, Int. J. Photoenergy 3 (2001) 1.